Eng. & Tech. Journal , Vol.30, No.18 ,2012

Vibration Analysis of Laminated Composites Using Experimental and Genetic Algorithms Optimization Technique

Dr. Nabil Hassan Hadi
Engineering College, University of Baghdad/Baghdad
Email:nabilhha@yahoo.com
Kayser Aziz Ameen
Engineering College, University of Baghdad/Baghdad
Email: kayseraziz@yahoo.com

Received on: 2/8/2011 & Accepted on: 3/5/2012

Abstract

In this paper, damage detection for different types of defects (delamination, crack and hole) in the composite laminate plate and cylindrical shell be used to characterize the vibration behavior experimentally which used two types of load (plus and sine load) to find the frequency response. To this end, some plates and cylindrical shells are made using hand-lay-up process. Glass fiber is used as a reinforcement in the form of bidirectional fabric and general purpose polyester resin as matrix for the composite material of plates and cylindrical shells. From the results, the damage detection by using the Genetic algorithms is investigated. Also, these experiments are used to validate the results of free vibration obtained from the finite elements program.

Keywords : Composite plate and shallow shell, Genetic algorithms, Damage detection, Dynamics tests, Natural frequency.

تحليل الاهتزازات للمواد المركبة باستعمال الطرق العملية وتقنية الخورزمية الجينية المثلى

الخلاصة

في هذه الدراسة، تم ايجاد الضرر لمختلف انواع العيوب (الانخلاعات، الشقوق و الثقوب) في الصقائح والرقائق قليلة الارتفاع المركبة بواسطة استعمال الخواص الاهتزازيةعملياً حيث تم استخدام نوعين من الاحمال (احمال نبضية و جيبية) لايجاد استجابة التردد. حيث تم صناعة الصفائح والرقائق بواسطة اليد ولقد تم استخدام الالياف الزجاجية كمدعم للصفائح وللرقائق المركبة اما مادة الترابط فقد تم استخدام مادة البولستر. تم استخدام الجينات الخوارزمية لتحديد مكان الضرر في الصفائح والرقائق قليلة الارتفاع كما تم حساب الترددات الطبيعية للهياكل عملياً وتم مقارنتها مع نتائج محسوبة بطريقة العناصر المحددة.

INTRODUCTION

In the recent decades the use of composite laminate materials on structural applications has been growing, requiring great effort on development of analysis and design techniques. The large number of design variables and complexity of the mechanical behavior are outstanding characteristics of composite material structures design. Such characteristics turn the project much more difficult and laborious than those involving conventional material. Optimization methods have been used in the sense of turn the composite material structural design a more systematic and well defined task. As alternative to gradient based methods, many

https://doi.org/10.30684/etj.30.18.7
2412-0758/University of Technology-Iraq, Baghdad, Iraq

other techniques were tested, having the genetic algorithm (GA) stand out the others because it perfectly adjusts to the problem characteristics. GAs are probabilistic optimization methods that seek to minic the biological reproduction and natural selection process through random, but structured, operations. The design variable are coded as genes and grouped together on chromosomes strings that represent an organism.

Züleyha Aslan and Mustafa Şahin, 2008. studied the effect of the size of beneath delaminations has no significant on the critical buckling load and compressive failure load of E-glass/epoxy composite laminates with multiple large delaminations, a numerical and experimental study is carried out to determine the buckling load of rectangular composite plates, for the experiments (0º/90º/0º/90º)s oriented cross-ply laminated plates with multiple large delaminations and without delamination are produced by using hand lay up technique and the results are compare with results obtained by ANSYS 11.0 package and good agreement obtained. **Jocab L. Pelletier and Senthil S. Vel.,2006,** presented a methodology for the multi-objective optimization of laminated composite materials that is based on an integer-coded genetic algorithm. The fiber orientation and fiber volume fractions of the laminae are chosen as the primary optimization variables. Simplified micromechanics equations are used to estimate the stiffness and strength of each lamina using the fiber volume fraction and material properties of the matrix and fibers. The lamina stresses for thin composite coupons subjected to force and/or moment resultants are determined using the classical lamination theory and the first ply failure strength is computed using the Tasi-Wu failure criterion. **Kosuke Takahashi, et. al.,2007,** proposed new measuring method of multiple electrical resistance changes to perform statistical diagnosis. The proposed method measures electrical resistance changes of multiple segments in a beam although electrical interference must be considered when multiple voltages are charged at once. Next statistical diagnosis is performed on loading to the beam a delamination crack is detected by the change of relative relationship between multiple electrical resistance changes due to damage occurring. **M. R. Ghasemi and A. Ehsani,2007,** studied the optimum weight and cost of a laminated composite plate, the Tsai- Hill theory is used as the failure criterion and the theory of analysis was based on the Classical lamination theory. A newly type of genetic algorithm as an optimization technique with a direct use of real variables was employed. Yet, since the optimization via genetic algorithm is a long process and the major time is consumed through the analysis, Radial basis function Neural network was employed in predicting the output from the analysis. **Felipe Schaedler de Almedia and Armando Miguel Awruch, 2007,** presented an optimization technique, using a genetic algorithm, applied to plates and shell of laminate composite materials, two cases are analyzed. In the first case weight and central deflection of a plate under a transverse pressure load are minimized using as optimization variables thickness and the fiber angle of each layer. In the second case, the stiffness maximization of cylindrical shell, under a transverse pressure load, and with geometrically nonlinear behavior, is obtained using as optimization variable the fiber angle of each layer. **Shun Fa Hwang, et. al., 2009,** presented the method to identify the effective elastic constants of inhomogeneous composite plates is demonstrated. The proposed method is applied successfully to determine the effective elastic constants of a woven composite plate and two PCB's a systematical two step procedure is proposed to

make up the problem of missing natural frequencies or natural frequencies with large errors due to the limitation in the measurement. **C. K. Cheung, et. al., 2004** studied the failure mode experimentally for S2 glass/epoxy composite strips with center hole of a pin joint at various temperatures with the range of -60ºC and 125ºC for different lay up configurations each of 24 layers : [0º], [0º/90º], [45º/-45º] and [0º/45º/90º/-45º] and four different hole diameters : 1/8, 1/4, 3/8 and 1/2 , the results indicate that the failure of the joint is significantly affected by stacking sequence, temperature and hole size and they obtain the stiffness of the joint, increase with decreasing hole diameter or temperature. As expected the [0º] specimens have the highest average stiffness and strength whereas the [45º/-45º] specimens the lowest with remaining configurations fall somewhere in between. A finite element failure model based on the Tsai-Wu tensor theory and progressive damage evolution was also developed. **Wang Jiam Min and Chen Long Zhu, 2005,** proposed the damage detection method by using the increment of lateral displacement change (IOLDC) as the damage identification parameters this method based on the fact that the damage in different types of structural members has distinctive influence on the structural stiffness. **Vijay Babbar, et. al., 2005,** used three dimensional (3D) magnetic finite element analysis to simulate the magnetic flux leakage signal from a circular dent geometry with associated residual stresses. Strain distribution information around the dent was obtained from an earlier work using finite element structural modeling, the localize residual stresses were simulated by assigning appropriate value of magnetic anisotropy to the relevant magnetic regions. **Huijian Li, Changjun He, et. al., 2005,** presented experimental and numerical analysis for crack damage detection using a combination of global (changes in natural frequencies) and local (stain mode shape) vibration based analysis data as input in artificial neural network for location and severity prediction of crack damage in beam like structures. Finite element analysis has been used to obtain the dynamic characteristics of intact and damage cantilever steel beams for the first three natural modes. **N. S. Bajaba and K. A. Alnefaie, 2008,** developed a new technique by using the wavelet transforms for detection of multiple damage in structures (beams) which consider a cantilevered beam with single and multiple damage. The responses (mode shapes) were obtained numerically (using finite element analysis) and experimentally (using impact testing and experimental modal analysis), then wavelet transforms is used to detect and characterize these defects. **D. Huynh and D. Tran, 2005,** presented a method of structural damage detection using non-destructive vibration test. It uses the frequency response function (FRF) data and finite element modal of the virgin structure to construct and display damage location vector (DLV), it is shown that DLV can detect, locate and assess the extent of damage. **Nabil H. H. and Aveen A. A.,2009,** studied two type of beam (straight and curved beam) and used the genetic algorithms to detect and locate the damage using five objective function. The results demonstrated that the objective function based on change in natural frequency is best function. **Mohammed F. Aly, et.al., 2010,** Investigated the dynamic behavior experimentally for beam by using a woven fiber and study influence of fiber orientation on natural frequency. In this work study the localized and detection the damage in the plates and shallow cylindrical are investigated by measure the change in natural frequency using two type of solutions (numerical solution and experimental solution).

PRODUCTION OF THE LAMINATES SPECIMENS

Glass fiber is used as a reinforcement in the form of bidirectional fabric and general purpose polyester resin as matrix for the composite material of the laminates specimens. The steps of manufacturing the composite shell or plate using hand lay up process are described below.

Preparation of the Mould

The hand lay-up process as shown in Figure (1), is open molding technique. The surface of the mould is thoroughly cleaned to be ready for the use, by removing any dust and dirt from it as shown in the Figure (2a, 2b) for plate and cylindrical shell mould.

Application of the release agent

After the mould surface has been cleaned, the release agent is applied. Where, the mould surface is coated with a free wax using a smooth cloth. Then a film of Polyvinyl alcohol (PVA) is applied over the wax surface using sponge. PVA is a water soluble material and 15% solution in water is used. When water evaporates, a thin film of PVA is formed on the mould surface. PVA film is dried completely before the application of resin coat. This is very important as the surface of final article will be marred with partly dried PVA film otherwise release will not be smooth.

Preparation of the matrix martial

The matrix material is prepared using general purpose (GP) Polyester resin. Cobalt Octate (0.35% by volume of resin) is added to act as accelerator. Methyl ethyl kentone peroxide (MEKP) (1% by volume) is added to act as catalyst. Resin, accelerator and catalyst are thoroughly mixed. The use of accelerator is necessary because without accelerator resin does not cure properly. After adding the accelerator and catalyst to the polyester resin, it has left for some time so that bubbles formed during stirring may die out. The amount of added accelerator and catalyst is not high because a high percentage reduces gel time of polyester resin and may adversely affect impregnation.

Preparation of the reinforcement

E-glass woven roving of is used as a reinforcement. The fabrics are made of fibers oriented along two perpendicular directions: one is called the warp and the other is called the fill (or weft) direction. The fibers are woven together, which means the fill yarns pass over and under the warp yarns, following a fixed pattern. Figure (3) shows a plain weave where each fill goes over a warp yarn then under a warp yarn and so on. Glass fiber mats (woven-mat), used for making the laminated plate or shell are cut in (5) layers of required size.

Preparation of the laminated plate and cylindrical panel

To preparation of laminate plate, the first layer of mat is laid and resin is spread uniformly over the mat by means of a brush. The second layer of mat is laid and resin is spread uniformly over the mat by means of a brush. After second layer, to enhance wetting and impregnation, a teethed steel roller is used to roll over the fabric before applying resin. This process is repeated till all the five fabric layers are placed. No external pressure is applied while casting or curing because uncured matrix material can squeeze out under high pressure. This results in surface waviness (non-uniform thickness) in the model material. The casting is cured at room temperature for (4-5)

hours and finally removed from the mould to get a fine finished composite plate. To preparation the shallow cylindrical laminate, it follow the same way above but the layer are continuous and it be controller by the turning (every 10º) of the cylinder and stopping by gear breaker

MATERIALS AND EXPERIMENTAL TEST SPECIMENS

Calculate the volume fraction of composite

The volume fraction of the fiber and voids are calculated from the measured weights and densities of fiber, matrix and composite. The fiber weight fraction of the specimens is measured by burning out the resin of the composite material. In the burning test, four samples have nominal (3.1mm for five layers) thicknesses are cut in rectangular shape of (89.25X85.5)mm and the average of total weight of the samples are (38 gm). An electronic balance is used to measure the weight of the four samples of the tested woven fabric composite and the result specimens from burning process as shown in Figure (5). The average weight of the four samples is measure as (38 gm). The average density of the samples is found to be (1606.3773 Kg/m^3). After the burning process, the resin is removed from the composite and the average weighted of the remaining woven roving fiber becomes (22.75 gm). Then the fiber weight fraction of the composite material is calculated to be (59.86%) and the resin weight fraction is (40.14%). The avoid volume fraction n_v is calculated from the measured weights and densities of fiber, matrix and composite, by equation (1). It is found to be 9.28%.

$$n_v = 1 - \frac{\left(W_f / r_f\right) + \left(W_c - W_f / r_m\right)}{W_c / r_c} \qquad \ldots(1)$$

Where W_f, W_m and W_c are the weights of the fiber, matrix, and composite respectively. By using the densities of the fiber r_f, matrix r_m, and composite r_c, respectively, the fiber volume fraction n_v can be obtained by equation (2) (**Mohammed F. Aly, et.al., 2010)**.

$$r_c = r_f n_f + r_m n_m = r_f n_f + r_m \left(1 - n_f - n_v\right) \qquad \ldots(2)$$

Where n_f ,n_m and n_v are the volume fractions of the fiber, matrix and voids respectively. Using the relation of equation (2) the fiber volume fraction (n_f) is found (36.988%) according to the densities of fiber and matrix presented in Table (1).

Preparation of the test specimens

After the cure process, test specimens are cut from the sheet of five (5) ply laminate of the sizes (350mm X 350mm X 3.1mm) for plate and (320mm X 320mm X 3.1mm) for shallow cylinder by using a diamond impregnated wheel, cooled by running water as shown in Figure (6). All the test specimens are finished by abrading

the edges on a fin carborundum paper. The laminated plate is cut at axis angle (0º-90º).

Materials characterization

The mechanical properties of constituents of the test specimens, E-glass woven roving fibers and polyester matrix are listed in Table (1). The material elastic properties of the lamina of test specimens are determined experimentally. These properties are Young's moduli (E_1 – in direction 1, E_2 – in direction 2, E_3 – in direction 3), Poisson's ratios (υ_{12}, υ_{13}, and υ_{23}), in plane shear modulus (G_{12}) and transverse shear moduli (G_{13} and G_{23}) as referred in Figure (7). This figure defines the material principle axes for a typical woven fiber reinforced lamina. Axis 1 is along the fiber length and represents the longitudinal direction of the lamina; axes 2 and 3 represents the transverse in-plane and through the thickness directions respectively. The some of the elastic constants of the woven fabric composite material are experimentally estimated (E_1, E_2, u_{12}) and another are estimated by using the relations which are based on elastic constants of the unidirectional specimens then the Yung's modulus and the Poisson's ratio of the fill and warp directions are calculated by using the three-point bending test which conducted according to the ASTM D790-80 standard. The specimen dimension shown in Figure (8), and the interface strain meter which calculate the strain from program by computer. The elastic constants of the unidirectional composite are calculated using the simple rule of mixtures by the relations of equation (3) from (**Mohammed F. Aly, et.al., 2010**) and the results are listed in Table (2).

$$E_1 = E_f n_f + E_m (1-n_f)$$

$$E_2 = E_m \left[\frac{E_f + E_m + n_f (E_f - E_m)}{E_f + E_m - n_f (E_f - E_m)} \right]$$

$$u_{12} = u_f n_f + u_m (1-n_f)$$

$$u_{23} = u_f n_f + u_m (1-n_f) \left[\frac{1 + u_m - u_{12} \frac{E_m}{E_1}}{1 - u_m^2 + u_m u_{12} \frac{E_m}{E_1}} \right]$$

$$G_{12} = G_m \left[\frac{G_f + G_m + n_f (G_f - G_m)}{G_f + G_m - n_f (G_f - G_m)} \right]$$

$$G_{23} = \frac{E_2}{2(1+u_{23})} \qquad \ldots(3)$$

Where indices *m* and *f* denote matrix and fiber, respectively. After calculating elastic constant of the unidirectional composite, elastic constants of the woven fabric composite material are estimated by using the tensile test device and the relation of equation (4) from reference (**Mohammed F. Aly, et.al., 2010**) and the results are listed in Table (3).

$$\left[\frac{1}{E_1}\ \frac{E_1(u_{12}+u_{23}+u_{12}u_{23})+u_{12}^2E_2}{E_1+E_2(1+2u_{12})}\right]^{UD}=\left[\frac{u_{13}}{E_1}\right]^{WF}$$

$$\left[\frac{(1-u_{23}^2)E_1^2+E_1E_2(1+2u_{12}+2u_{12}u_{23})-u_{12}^2E_2^2}{E_1E_2(E_1+E_2(1+2u_{12}))}\right]^{UD}=\left[\frac{1}{E_3}\right]^{WF}$$

$$\left[\frac{1}{G_{12}}\right]^{UD}=\left[\frac{1}{G_{12}}\right]^{WF}$$

$$\left[\frac{1+u_{23}}{E_2}+\frac{1}{2G_{12}}\right]^{UD}=\left[\frac{1}{G_{13}}\right]^{WF} \quad \ldots(4)$$

Where indices UD and WF denote the unidirectional fiber and woven fiber respectively

TYPES OF DAMAGE STRUCTURE

The damage structures investigated in this work are in the form of simple plates and shallow cylindrical. The delamination damage representing by using but the aluminium foil between layers where the delamination size (8X8 cm)for plate and (6.5X6.5 cm) for cylinder, the crack representing by cut depth (0.51 mm) and length (6.5 cm) by using a diamond impregnated wheel and the last type of damage making a hole by using a drill the diameter of hole are (2.4 cm). The place of all damages on the center of the specimens.

EXPERIMENTAL MODAL ANALYSIS

Structural natural frequencies may be measured by applying steady state, random or shock loads to the structure. If shock loads are used (experimental setup I) then in this case it becomes necessary to determine the Fast Fourier Transforms (FFT) of the response of the structure and input force. While the steady state method (experimental setup II), the structures excited by a sine wave of constant amplitude and frequency. The two type which considering in this work.

Pulse load (Experimental setup I)

Through an impact experimental test, it is determined the frequency response functions which relate the response given by the specimen when loaded with a signal, allowing for the determination of the natural frequencies, the impact hammer is used to give the input load (pulse) to the specimen, and the signal is analyzing by using wave record command and the Fast Fourier Transform (FFT) in Matlab program, see the flowchart in bellow, can be obtain the natural frequencies. The block diagram of the different instruments that used for the measurements of natural frequencies is shown in Figure (9), and the model setup of this experimental.

Sine load (Experimental setup II)

The block diagram shows all the instruments that used in the experimental as shown in Figure (11). A shaker was seated at appropriate position to excite the model. This shaker was driven through a power amplifier by a sinusoidal signal generator. The response was measured using a mini accelerometer and displayed on an oscilloscope through a charge amplifier. Figure (12) shows the instrumentation set up.

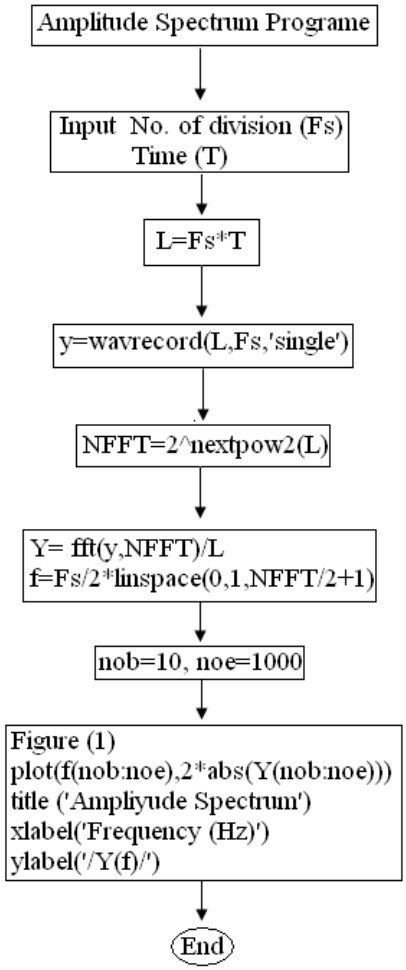

The flowchart of the programs for the experimental setup (I).

DAMAGE DETECTION METHOD

Damage detection by means of non-destructive testing plays an important role in ensuring the integrity of structures. These techniques are based on the monitoring of changes in dynamic structural characteristics such as natural frequencies and mode shape. The identification damage is formulated as an optimization problem where the basic procedure is to find a set of damage parameters that yields the optimum correlation between the numerical model and the measured model. The GAs theory is used to find the optimal solution by minimizing or maximize the objective functions, the GA begins by defining a chromosome, (i.e. an

array of variables whose values are to be optimized). In the present work the chromosome has two variables, the damage location and the stiffness reduction. The objective function generates an output from the set of input variables of a chromosome. The goal is to modify the output in some desirable fashion by finding the appropriate values of input
variables. Figure (13) shows the block diagram of the method of damage detection using genetic algorithms. The natural frequency used as a diagnostic parameter in structural assessment procedures using vibration monitoring. One great advantage of using only eigenvalue in the damage assessment of structures is that they are cheaply acquired and the approach can give an inexpensive structural assessment technique,

Parameter of GA

The free vibration of (SSSS) and (CCCC), plate and (CFCF) cylindrical with and without damage is performed. Model responses of the plate and cylindrical are generated using finite element model. The material properties of the laminated composite are listed in Table (4), and Figures (14,15) demonstrate the dimensions of plate and cylindrical respectively. For GA, the values of some parameters need to be selected. These parameters are listed in Table (4).

RESULTS AND DISCUSSION

The deviations of the numerical results and experimental and between two experimental methods, some possible measurement errors can be pointed out such as: measurement noise, positioning of the accelerometers and their mass, non-uniformity in the specimens properties (voids, variations in thickness, non uniform surface finishing). Such factors are not taken into account during the numerical analysis, since the model considers the specimen entirely perfect and with homogeneous properties, what rarely occurs in practice. Another aspect to be considered is that the input properties in the model came from the application of the rule of mixture and they do not take into account effects of fiber matrix interface as well as the irregular distribution of resin on the fibers. Also, these models did not include damping effects, which can have a large influence on the structure behavior. Also the computational numerical program does not allow for the consideration of fibers interweaving present in the fabric used.

Calculate The Natural Frequency

Plate and cylindrical shell

Tables (5,6,7,8,9,10,11,12) give the comparison of the first five mode of natural frequency between experimental work and numerical work by used the program and results in reference **Nabil Hassan Hadi and Kayser Aziz Ameen**, **2011** for five woven laminated plate with different type of defect and different boundary conditions of $[0/90]_5$ laminated. Also the results can be show in the Figure (16 to 23). The average errors between the experimental setup I, experimental setup II and numerical solution respectively with (CCCC) and (SSSS) boundary condition respectively was (15.5222%, 6.68534%), and (15.506%, 7.1126%) for intact case, (10.3569%, 13.4196%) and (6.176%, 11.56%) for delamination case, (4.7519%%, 14.80645%) and (8.541%, 21.638%) for crack case and (11.66078%, 6.685348%) and (11.661%, 11.042%) for hole case. Also from these Tables good agreements between the experimental setup I, and experimental setup II for different boundary condition

((CCCC) and (SSSS)) noted the average errors was (8.498%, 6.685%) for intact case, (8.553%,7.786%) for delamination case, (9.1011%, 7.86%)for crack case and 97.954%, 9.387%) for hole case respectively. Tables (13,14,15,16) give the comparison of the first five mode of natural frequency between experimental setup (I) and numerical work for five woven laminated cylindrical shell with different type of defect for clump free clump free (CFCF) boundary conditions of $[0/90]_5$ woven laminated. The results show, with average errors (12.43921%) for intact case, (12.24938%) for delamination case, (17.52105%) for crack case and (13.51321%) for hole case. Figure (24, 25, 26 and 27) show the result obtained by using the experimental setup (I).

The deviations of the numerical results and experimental and between the two experimental methods are due to some possible measurement errors that can be pointed out such as: measurement noise, different positioning of the accelerometers and their mass, non-uniformity in the specimens properties (voids, variations in thickness, non uniform surface finishing). Such factors are not taken into account during the numerical analysis, since the model considers the specimen entirely perfect and with homogeneous properties, which rarely occurs in practice. Another aspect to be considered is that the input properties in the model came from the application of the rule of mixture and they do not take into account effects of fiber matrix interface as well as the irregular distribution of resin on the fibers. Also, the computational numerical program does not allow for the consideration of fibers interweaving present in the fabric used.

Damage Detection

The natural frequency used as a diagnostic parameter in structural assessment procedures using vibration monitoring. One great advantage of using only eigenvalue in the damage assessment of structures is that they are cheaply acquired and the approach can give an inexpensive structural assessment technique. The objective function to be maximized is defined as follows.

$$\Delta w = \sum_{i}^{n} \left(w_i^m - w_i^a \right)^{2`} \qquad \text{.....(5)}$$

Where :

i :- Mode number (i=1,2,3,…..,n)

w_i^m :-Test natural frequencies

w_i^a :-Calculated natural frequencies

The w_i^m are the natural frequencies which are applied to our damage detection system as inputs. An objective value of zero indicates an exact match between the values of frequencies. The first natural frequencies are calculated numerically using finite element model for the test damage element of the simply supported and clamp for all side respectively for plate and clamp-free-clamp-free for shallow cylindrical to three damage cases (delamination, crack and hole).These frequencies were used as test input for GA. After introducing the test natural frequencies, a population of individuals is generated randomly and the natural frequencies are calculated for each chromosome, which coded the damage state, then the objective function equation (5) is evaluated for these chromosomes. Only best chromosomes are selected to continue, and reproduction and mutation operator are applied on the chromosomes except the

best chromosome. After mutation operator one generation is completed and in the next generation the new population is used for calculating the natural frequencies and cost evaluation. The best cost value is checked in every generation and if the cost reaches a certain level. The convergence plot for the GA for plate and simply support boundary condition for all side are shown in Figure (28), it is seen that convergence occurs at a round (3) for delamination case, (6) for crack case and (8) for hole. The convergence plot for the GA for plate and clamp boundary condition for all side are shown in Figure (29), it is seen that convergence occurs at a round (12) for delamination case, (10) for crack case and (7) for hole. The convergence plot for the GA for cylindrical and clamp-free-clamp-free boundary condition each side respectively are shown in Figure (30), it is seen that convergence occurs at a round (3) for delamination case, (8) for crack case and (5) for hole.

CONCLUSIONS

The main conclusions that can be draw from this investigation are:

- Results show that Genetic Algorithm is an efficient method in damage identification for different boundary condition of structure with high precision and capable of detecting small damage with small errors.
- The length of the run (in term of generation number) and results depends on the initial randomly generated population and GA parameters and the test point.
- When the plate or shell containing some defect such as delamination, crack or hole this causes a decreasing in natural frequency, this properties used to detecte the damage in structure.
- Single and multiple damages can be detected in plate or in shell by using the genetic algorithms.

REFERENCES

[1]Züleyha Aslan and Mustafa Şahin, "Buckling Behavior and Compressive Failure of Composite Laminates Containing Multiple Large Delaminations", Journal of Composite Structures, Vol. (89), pp. 382-390, September 2008.

[2]Jocab L. Pelletier and Senthil S. Vel, "Multi-Objective Optimization Of Fiber Reinforced Composite Laminates For Strength, Stiffness and Minimal Mass", Journal of Computers & Structures, Vol. (84), pp. 2065-2080, September 2006.

[3]Kosuke Takahashi, Akira Todoroki, Yoshinobu Shimamura and Atsushi Lwasaki, "Statistical Damage Detection of Laminated CFRP Beam Using Electrical Resistance Change Method", Journal of Key Engineering Materials, Vol. (353), No. (358), pp. 1330-1333, 2007.

[4]M. R. Ghasemi and A. Ehsani, "Multi- Objective Optimization of Composite Laminates Under Heat And Moisture Effects Using a Hybrid Neuro- Genetic Algorithm", Journal of World Academy of Science, Engineering and Technology, Vol. (21), pp. 187-192, January 2007.

[5]Felipe Schaedler de Almedia and Armando Miguel Awruch, "Optimization Of Composite Plates And Shells Using A Genetic Algorithm And The Finite Element Method", Journal of de Mecànica Computacional, Vol. (XXVI), pp. 372-385, October 2007.

[6]Shun Fa Hwang, Jen Chih Wu and Rong Song He, "Identification Of Effective Elastic Constants Of Composite Plates Based On A Hybrid Genetic Algorithm", Journal of Composite Structures, Vol. (90), pp. 217-224, April 2009.
[7]C. K. Cheung, B. M. Liaw, F. Delale and B. B. Raju, "Composite Strips With A Circular Stress Concentration Under Tension", International Congress and Exposition on Experimental and Applied Mechanics, Costa Mesa, CA, Paper No. 387, June 2004.
[8]Wang Jiam Min and Chen Long Zhu, "Damage Detection Of Frames Using The Incremental Of Lateral Displacement Change", Journal of Zhejiang University Science, Vol. (6A), No. (3), pp. 202-212, 2005.
[9]Vijay Babbar, James Bryne and Lynann Clapham, "Mechanical Damage Detection Using Magnetic Flux Leakage Tools: Modeling The Effect Of Dent Geometry And Stresses", Journal of NDT&E International, Vol. 38), pp. 471-477, December 2005.
[10]Huijian Li, Changjun He, Hui Wang and Caizhe Hao, "Crack Damage Detection In Beam Like Structures Using RBF Neural Networks With Experimental Validation", Journal of International Innovative Computing, Information and control, Vol. (1), No. (4), December 2005.
[11]N. S. Bajaba and K. A. Alnefaie, "Multiple Damage Detection In Structures Using Wavelet Transforms", Journal of Emirates Engineering Research, Vol. (10), No. (1), pp. 33-40, March 2005.
[12]D. Huynh and D. Tran, "A Non- Destructive Crack Detection Technique Using Vibration Tests", Journal of Structural Integrity and Fracture, Vol. (27), No. (2),2005.
[13]Aveen A. abdul, "Damage Detection and Assessment in Mechanical Beams Using Genetic Algorithm", Baghdad University, M.Sc. Thesis, May 2009.
[14]Mohammed F. Aly, I. G. M. Goda, and Gala A. Hassan, "Experimental Investigation of the Dynamic Characteristics of Laminated Composite Beams", international Journal of Mechanical & Mechatronics IJMME-IJENS, Vol. 10, No. 3, pp. 59-68, 2010.
[15] ASTM, D 790-80. "Standard Test Method for Flexural Properties of Plastics and Electrical Insulating Materials", American Society for Testing and Materials, 1981.
[16]Nabil Hassan Hadi and Kayser Aziz Ameen, "Nonlinear Free Vibration Of Cylindrical Shells With Delamination Using High Order Shear Deformation Theory :-A Finite Element Approach", American journal of Scientific and industrial Research, Vol. 2, Issue No. 2, pp. 251-277,2011.

Table (1) Mechanical properties of Fiber and resin.

Material	Properties	Value
E-Glass fiber	Elasticity modulus (GPa)	74
	Shear modulus (GPa)	30
	Density (kg/m^3)	2600
	Poisson ratio	0.25
Polyester resin	Elasticity modulus (GPa)	4.0
	Shear modulus (GPa)	1.4
	Density (kg/m^3)	1200
	Poisson ratio	0.4

Table (2). Mechanical properties of unidirectional composite material.

Properties	Value
Elastic modulus (E_1) (GPa)	29.8916
Elastic modulus (E_2) (GPa)	7.975036
Shear modulus in plane 1-2 (G_{12}) (GPa)	2.822
Shear modulus in plane 2-3 (G_{23}) (GPa)	2.5836
Poisson ratio in plane 1-2 (u_{12})	0.3445
Poisson ratio in plane 2-3 (u_{23})	0.543

Table (3). Mechanical properties of woven composite material.

Properties	Value
Elastic modulus (E_1=E_2) (GPa)	14.10782
Elastic modulus (E_3) (GPa)	9.2785889
Shear modulus in plane 1-2 (G_{12}) (GPa)	1.5879425
Shear modulus in plane 1-3 (G_{13}) (GPa)	2.6978
Shear modulus in plane 3-3 (G_{23}) (GPa)	2.6978
Poisson ratio in plane 1-2 (u_{12})	0.1036
Poisson ratio in plane 1-3 (u_{13})	0.36
Poisson ratio in plane 2-3 (u_{23})	0.36

Table (4). Parameters of GA.

Parameter	value
Population size	50
Number of Elitism	2
Crossover probability P_c	0.96
Mutation probability P_m	0.02

Table (5). Comparison between experimental work and numerical results for five woven layers laminated intact plate ($[0/90]_5$), with (CCCC) boundary condition.

Mode No.	Experimental setup (I) (Hz)	Experimental setup (II) (Hz)	Numerical result (Hz)	Discrepancy percentage between numerical & I (%)	Discrepancy percentage between numerical & II (%)	Discrepancy percentage between two experimental (%)
1	262.501	250	250.22	4.90799	0.08804	4.762304
2	475.002	405	559.924	15.1667	27.6688	14.73722
3	737.502	670	799.892	7.79974	16.2386	9.152826
4	903.125	905	1183.42	23.685	23.5266	0.207612
5	1012.05	1150	1369.2	26.0518	10.0095	13.63075
Average error (%)				15.52224	15.5063	8.498142

Table (6). Comparison between experimental work and numerical results for five woven layers laminated plate ($[0/90]_5$), with delamination and (CCCC) boundary condition.

Mode No.	Experimental setup (I) (Hz)	Experimental setup (II) (Hz)	Numerical result (Hz)	Discrepancy percentage between numerical & I (%)	Discrepancy percentage between numerical & II (%)	Discrepancy percentage between two experimental (%)
1	248.276	235	231.209	7.38145	1.63955	5.347199
2	444.828	380	405.397	9.7264	6.26471	14.57363
3	724.138	655	580.011	24.849	12.9289	9.547615
4	832.372	830	864.298	3.69385	3.96829	0.284957
5	937.931	1060	999.221	6.1338	6.08261	13.01471
Average error (%)				10.3569	6.176811	8.553621

Table (7). Comparison between experimental work and numerical results for five woven layers laminated plate ($[0/90]_5$), with crack and (CCCC) boundary condition.

Mode No.	Experimental setup (I) (Hz)	Experimental setup (II) (Hz)	Numerical result (Hz)	Discrepancy percentage between numerical & I (%)	Discrepancy percentage between numerical & II (%)	Discrepancy percentage between two experimental (%)
1	245.454	230	225.256	8.966	2.10623	6.296088
2	466.661	390	458.575	1.763	14.9539	16.42756
3	618.18	560	626.451	1.320	10.6076	9.411513
4	724.24	720	778.828	7.009	7.55342	0.585455
5	957.575	1080	1004.8	4.700	7.48397	12.7849
Average error (%)				4.751	8.5410	9.1011

Table (8). Comparison between experimental work and numerical results, for five woven layers laminated plate ($[0/90]_5$), with hole (CCCC) boundary condition.

Mode No.	Experimental setup (I) (Hz)	Experimental setup (II) (Hz)	Numerical result (Hz)	Discrepancy percentage between numerical & I (%)	Discrepancy percentage between numerical & II (%)	Discrepancy percentage between two experimental (%)
1	232.923	220	217.427	7.12719	1.18357	5.548185
2	440.077	375	435.399	1.07433	13.8722	14.78762
3	600.072	540	611.141	1.81123	11.6407	10.01078
4	907.692	900	708.108	28.1856	27.0993	0.847457
5	1013.08	1100	1052.55	3.74996	4.50819	8.579884
Average error (%)				8.3896	11.6607	7.95478

Table (9). Comparison between experimental work and numerical results, for five woven layers laminated intact plate ($[0/90]_5$), with (SSSS) boundary condition.

Mode No.	Experimental setup (I) (Hz)	Experimental setup (II) (Hz)	Numerical result (Hz)	Discrepancy percentage between numerical & I (%)	Discrepancy percentage between numerical & II (%)	Discrepancy percentage between two experimental (%)
1	135.2045	120	119.1384	13.4852	11.2455	11.2455
2	320.1219	310	324.6359	1.39048	3.16188	3.16188
3	480.0331	420	490.5194	2.13779	12.5060	12.5060
4	610.1589	590	724.2334	15.7510	3.30387	3.30387
5	750.0977	710	857.3053	0.66215	5.34566	5.34566
Average error (%)				6.68534	7.11260	7.11260

Table (10). Comparison between experimental work and numerical results for five woven layers laminated plate ([0/90]), with delamination and (SSSS) boundary condition.

Mode No.	Experimental setup (I) (Hz)	Experimental setup (II) (Hz)	Numerical result (Hz)	Discrepancy percentage between numerical & I (%)	Discrepancy percentage between numerical & II (%)	Discrepancy percentage between two experimental (%)
1	129.201	115	106.408	21.421	8.075088	10.9914
2	295.011	280	252.722	16.7335	10.79363	5.08841
3	430.257	380	405.374	6.13821	6.25940	11.6806
4	550.671	520	618.344	10.9442	15.90441	5.56976
5	741.562	700	841.355	11.861	16.80089	5.60465
Average error (%)				13.4196	11.566687	7.78698

Table (11). Comparison between experimental work and numerical results for five woven layers laminated plate ($[0/90]_5$), with crack and (SSSS) boundary condition.

Mode No.	Experimental setup (I) (Hz)	Experimental setup (II) (Hz)	Numerical result (Hz)	Discrepancy percentage between numerical & I (%)	Discrepancy percentage between numerical & II (%)	Discrepancy percentage between two experimental (%)
1	95.62103	80	111.0914	13.9258034	27.98722	16.3364
2	218.0221	210	302.385	27.8991683	30.55211	3.679489
3	430.3872	380	470.7881	8.58154656	19.28428	11.70741
4	610.2789	600	701.0371	12.9462763	14.41251	1.684295
5	701.4431	660	785.3098	10.6794414	15.95673	5.908263
Average error (%)				14.806447	21.6385	7.863171

Table (12). Comparison between experimental work and numerical results for five woven layers laminated plate ($[0/90]_5$), with hole and (SSSS) boundary condition.

Mode No.	Experimental setup (I) (Hz)	Experimental setup (II) (Hz)	Numerical result (Hz)	Discrepancy percentage between numerical & I (%)	Discrepancy percentage between numerical & II (%)	Discrepancy percentage between two experimental (%)
1	125.0235	100	110.1671	13.48524	9.228872	20.01504
2	210.0113	210	212.9726	1.390480	1.395786	0.005381
3	430.9811	380	440.3958	2.137795	13.71399	11.82908
4	570.0014	550	676.5681	15.75106	18.70737	3.509009
5	780.3486	690	785.5501	0.662152	12.16346	11.57798
Average error (%)				6.68534	11.0418	9.38729

Table (13). Comparison between experimental work and numerical results for five woven layers laminated intact shallow cylindrical shell ($[0/90]_5$), with (CFCF) boundary condition.

Mode No.	Experimental setup (I) (Hz)	Numerical result (Hz)	Errors%
1	162.16216	166.3283	2.504769182
2	254.05405	326.3512	22.15317425
3	562.1622	659.1854	14.71865123
4	664.8648	774.9573	14.20626659
5	891.8918	821.1635	8.613181175
Average error (%)			12.439208485%

Table (14). Comparison between experimental work and numerical results for five woven layers laminated delamination shallow cylindrical shell ($[0/90]_5$), with (CFCF) boundary condition.

Mode No.	Experimental setup (I) (Hz)	Numerical result (Hz)	Errors%
1	150.35135	149.214056	0.762189589
2	221.62162	294.6893471	24.79483152
3	454.0548	542.4198158	16.29089005
4	556.75675	658.9480384	15.50824684
5	751.35135	781.7681094	3.890764928
Average error (%)			12.249384585%

Table (15). Comparison between experimental work and numerical results for five woven layers laminated crack shallow cylindrical shell ($[0/90]_5$), with (CFCF) boundary condition.

Mode No.	Experimental setup (I) (Hz)	Numerical result (Hz)	Errors%
1	156.75673	153.784	1.933055454
2	216.2616	271.8040054	20.4347266
3	318.9189	468.9609007	31.99456511
4	475.6756	654.440961	27.31573536
5	702.7027	746.9773672	5.927176531
Average error (%)			17.521051811

Table (16). Comparison between experimental work and numerical results for five woven layers laminated hole shallow cylindrical shell ($[0/90]_5$), with (CFCF) boundary condition.

Mode No.	Experimental setup (I) (Hz)	Numerical result (Hz)	Errors%
1	151.35135	150.2397474	0.739885829
2	227.027	299.6329572	24.23163255
3	486.4865	590.4488813	17.60734665
4	601.01201	730.531363	17.72947193
5	859.4595	801.3031279	7.257724328
Average error (%)			13.513212257

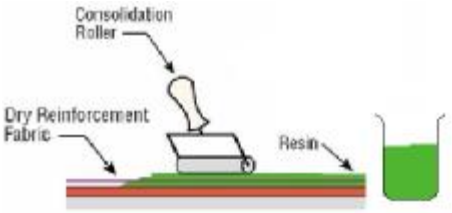

Figure (1). Hand lay-up technique

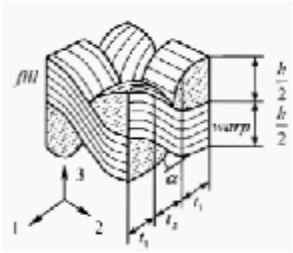

Figure (3) Schematic representation of woven fabric architecture

-A-

-B-

Figure (2). Model of mould (A) The plate mould. (B) The cylindrical mould

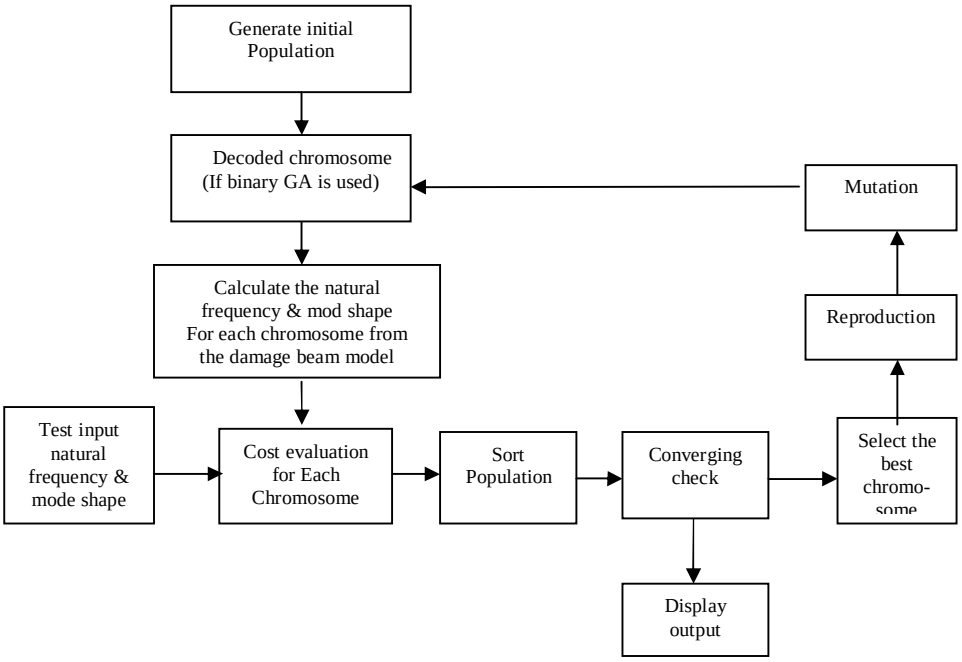

Figure (4)Charge amplifier for Accelerometer (7)Oscilloscope.

Figure (5). The woven fiber composite after burning process.

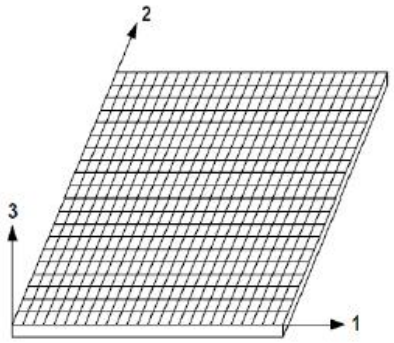

Figure (7). Lamina reference.

-*A*-

-B-

Figure (6). The specimens of (A) plate (B) cylindrical shell.

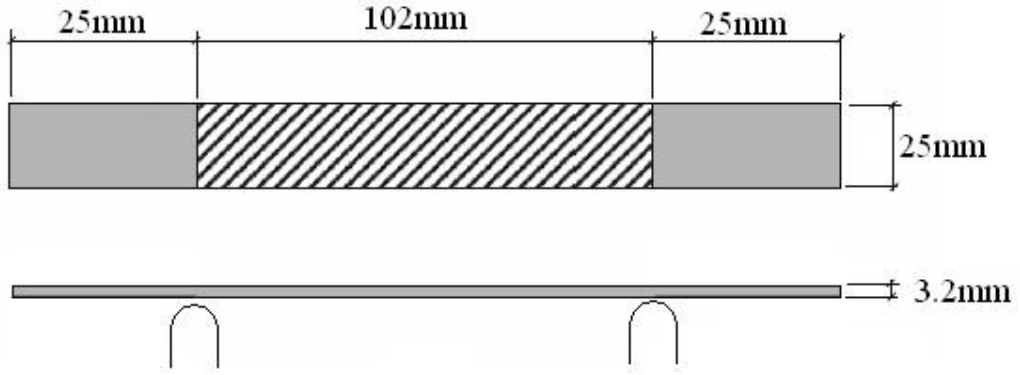

Figure (8). The specimen dimension.

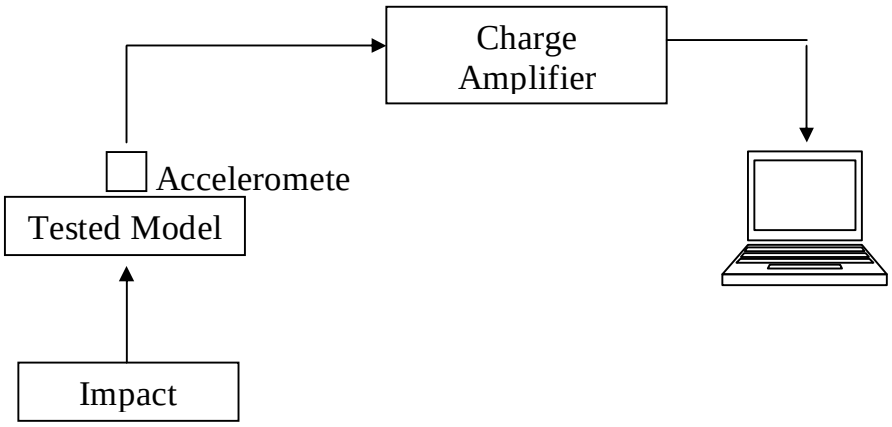

Figure (9). Block diagram for testing elements used in measuring natural frequencies (Experimental setup I).

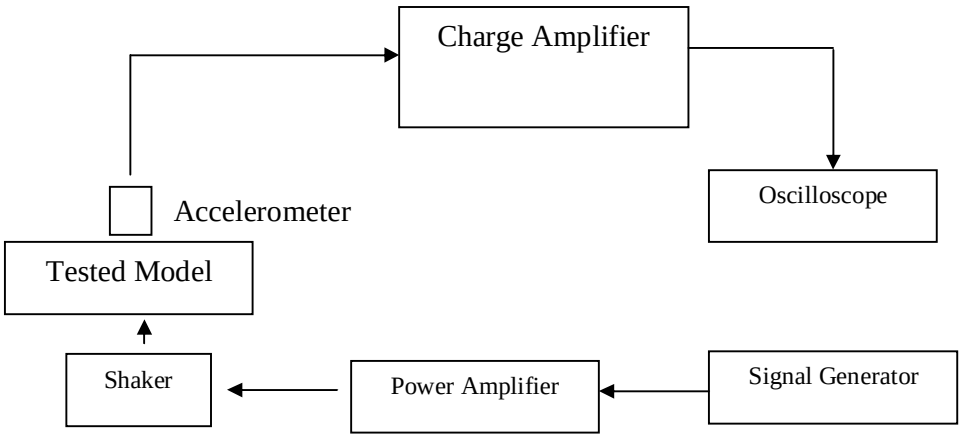

Figure (11). Block diagram for measuring natural frequencies (Experimental setup II).

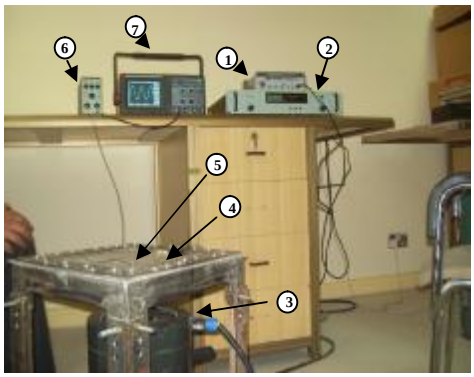

Figure (12).Model II set up for modal testing of a laminated plate (1)Sign generator (2)Charge amplifier for sign generator (3) Shaker (4)Tested modal (5)Accelerometer (6)Charge amplifier for Accelerometer (7)Oscillosco.

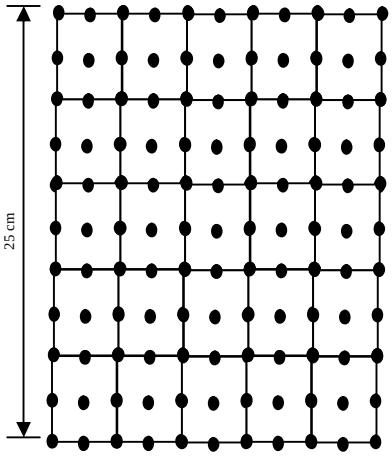

Figure (14). Mesh generation and dimensions of the plate.

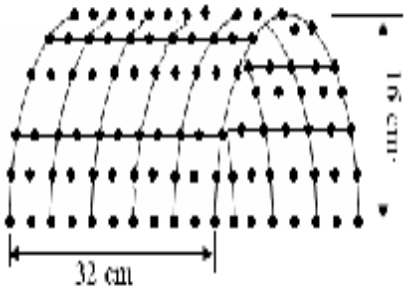

Figure (15). Mesh generation and dimensions of cylindrical shell.

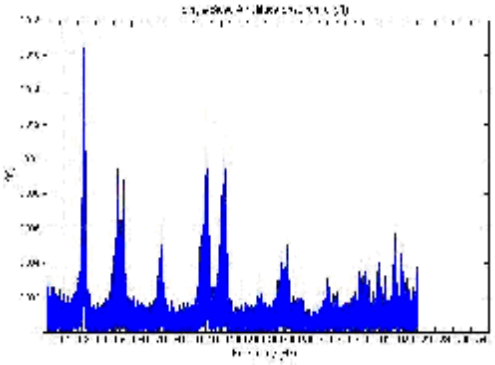

Figure (16). Results for experimental setup (I), for woven laminated (CCCC) intact plate, |Y(f)| is the response.

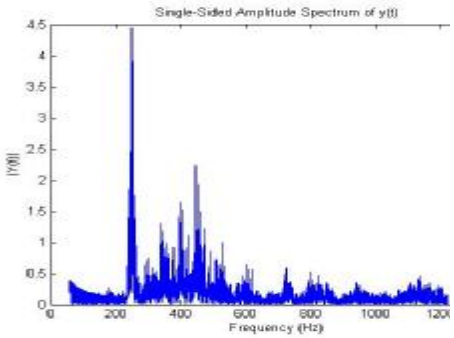

Figure (17). Results for experimental setup (I), for woven laminated (CCCC) plate with delamination, |Y(f)| is the response.

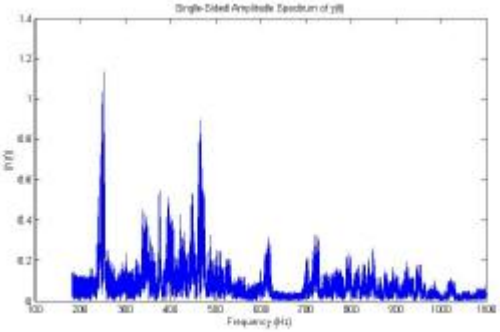

Figure (18). Results for experimental setup (I), for woven laminated (CCCC) plate with crack, |Y(f)| is the response.

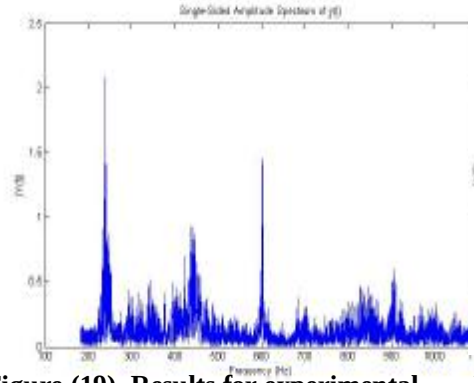

Figure (19). Results for experimental setup (I), for woven laminated (CCCC) plate with hole, |Y(f)| is the response.

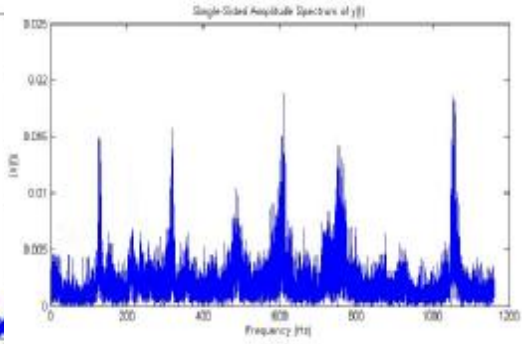

Figure (20). Results for experimental setup (I), for woven laminated (SSSS) intact plate, |Y(f)| is the response.

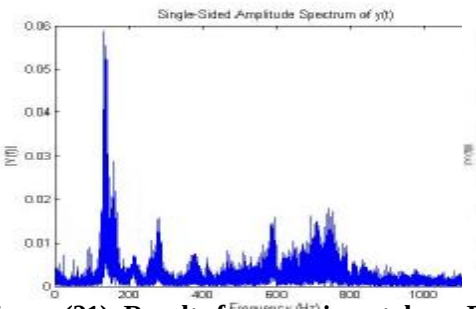

Figure (21). Results for experimental setup (I), for woven laminated (SSSS) plate with delamination, |Y(f)| is the response.

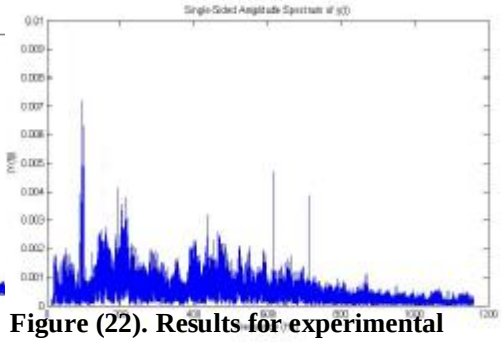

Figure (22). Results for experimental setup (I), for woven laminated (SSSS) plate with crack, |Y(f)| is the response.

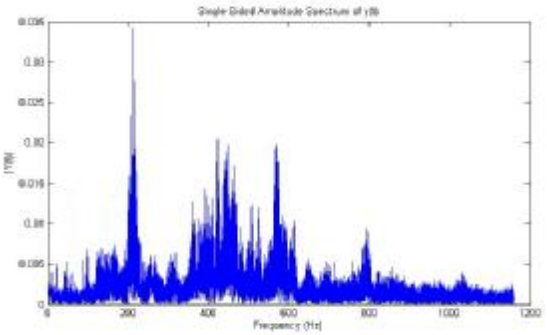

Figure (23). Results for experimental setup (I), for woven laminated (SSSS) plate with hole, |Y(f)| is the response.

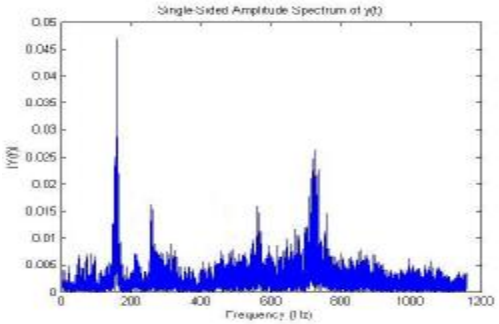

Figure (24). Results of experimental setup (I), for woven laminated intact cylindrical shell for (CFCF) boundary condition.

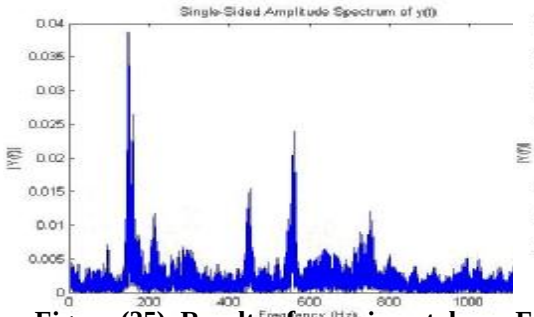

Figure (25). Results of experimental setup (I), for woven laminated cylindrical shell for (CFCF) boundary condition with delamination.

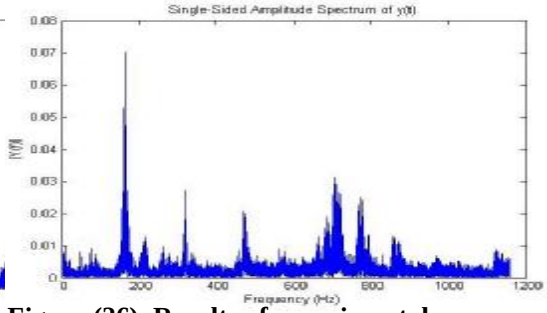

Figure (26). Results of experimental setup (I), for woven laminated cylindrical shell for (CFCF) boundary condition with crack.

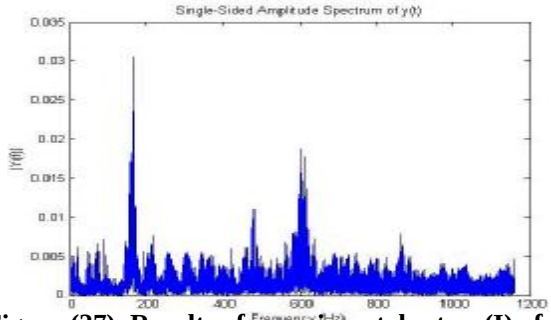

Figure (27). Results of experimental setup (I), for woven laminated cylindrical shell for (CFCF) boundary condition with hole, |Y(f)| is the response.

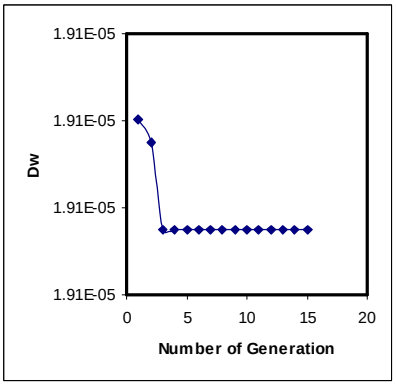

-*A*-

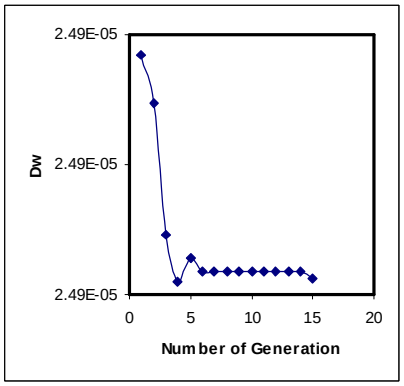

-B-

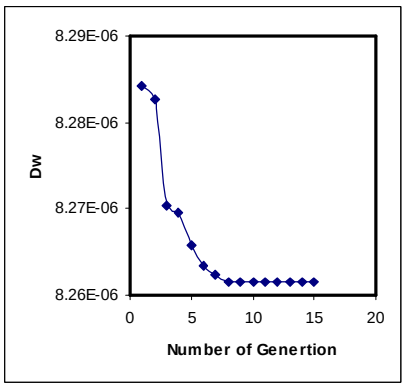

-*C*-

Figure (28). A typical objective function curve of GA convergence for simply supported plate (A) delamination (B) crack (C) hole

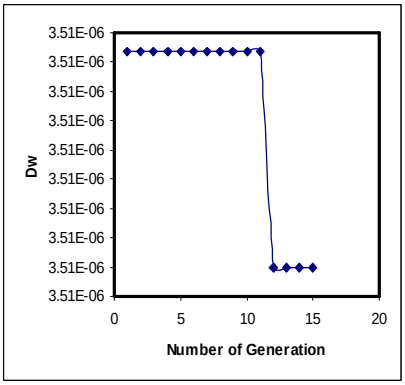

-*A*-

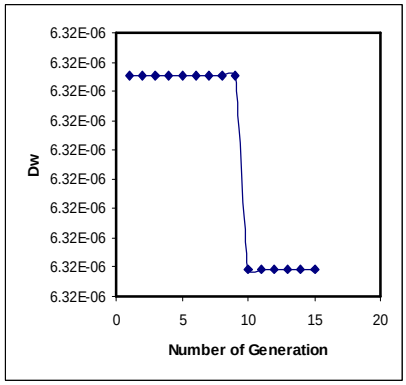

-B-

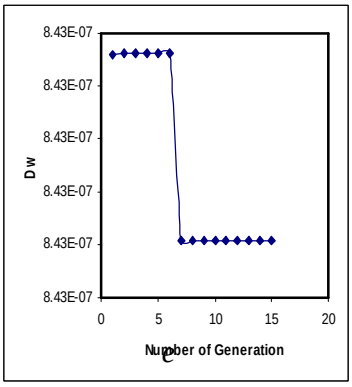

-*C*-

Figure (29). A typical objective function curve of GA convergence for clamp plate (A) delamination (B) crack (C) hole.

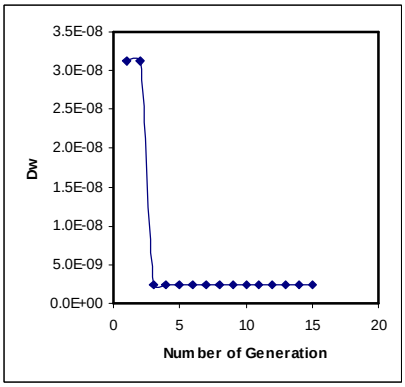

-*A*-

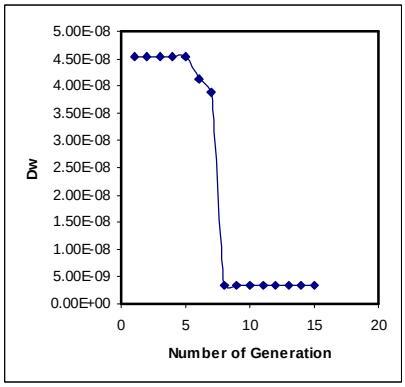

-B-

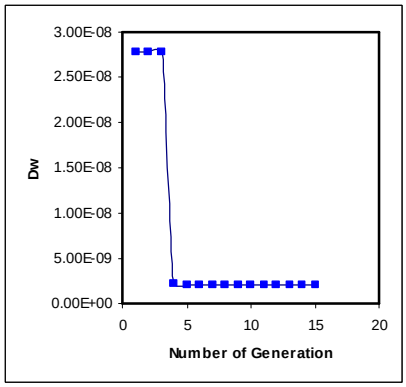

-*C*-

Figure (30). A typical objective function curve of GA convergence for cylindrical shell (CFCF) (A) delamination (B) crack (C) hole